

# Analysis and design of all-optical 1-bit binary full adder employing microring resonator

BHUVANESWARI VISWANATHAN<sup>1</sup>, YUVARAJ SIVAGNANAM<sup>2</sup>, JAYANTA KUMAR RAKSHIT<sup>3</sup>,  
MANJUR HOSSAIN<sup>4,\*</sup>

<sup>1</sup>*Department of Electronics and Communication Engineering, SRM Institute of Science and Technology, City Campus, Vadapalani, Chennai-600026, Tamil Nadu, India*

<sup>2</sup>*Department of Electronics and Communication Engineering, SRM Institute of Science and Technology, SRM Nagar, Kattankulathur, Chennai-603203, Tamil Nadu, India*

<sup>3</sup>*Department of Electronics and Instrumentation Engineering, National Institute of Technology Agartala, Agartala, 799046, India*

<sup>4</sup>*Department of Computer Science and Engineering, Saveetha Institute of Medical and Technical Sciences, Chennai, 602105, India*

Proposed manuscript includes the analysis and design of compact all-optical 1-bit binary full adder using microring resonator. Large-scale optical integrated circuits are being taken into account as a substitute for conventional CMOS technology in the field because to the growing demand for ultra-fast terahertz data transfer and processing. Furthermore, circuits that use less energy are becoming more and more important. The architecture is designed and analyzed at about 260 Gbps using MATLAB. The proposed design is simulated also in "Ansys Lumerical finite difference time domain (FDTD)" software. The footprint of the design in FTDD is only  $34.1 \times 32.2 \mu\text{m}^2$ . This proposed 1-bit full adder is particularly useful for digital signal processing because of its small architecture and faster response times. The evaluation and analysis of a few performance-indicating variables includes "extinction ratio", "contrast ratio", "amplitude modulation", "on-off ratio", "quality factor", "photon cavity lifetime", and "relative eye opening". Optimized design parameters chosen to implement the design practically.

(Received July 30, 2024; accepted February 3, 2025)

*Keywords:* All-optical switch, Full adder, Microring resonator (MRR), FDTD

## 1. Introduction

Data rates approaching terabits per second are being investigated by researchers due to the advancement of contemporary digital signal processing and communication networks. The promise of optical processing has encouraged a lot of recent efforts to get over fundamental performance limitations of semiconductor devices, which include considerable heat generation and inherent delay. The transition from conventional carrier electron to photon is required in devices intended for logic and switching operations in order to achieve high data rates. All-optical (AO) approaches have been the subject of extensive research and development in the photonics sector during the past few decades. This includes different kinds of designs, algorithms, and mathematical and logical procedures. Recently developed AO technologies are "Mach Zehnder interferometer (MZI)", "semiconductor-optical amplifier (SOA)", "quantum-dot SOA (QD-SOA)", "terahertz-optical asymmetric de-multiplexers (TOAD)", "non-linear material (NLM)" and "microring resonator (MRR)" etc. [1-11] which are utilized to implement various logic circuits.

One of the most important mathematical operations for creating a central processing unit is the sum operation. A variety of photonics technologies were examined by researchers in an effort to develop an all-optical full adder (FA). Two-dimensional photonic crystal (PhC) has been used to implement 1-bit FA [12-14]. AO 1-bit FA has been shown using MZI based on SOA [15-16]. Also, AO 1-bit FA has been developed using MRR with 100 Gbps data rate only [17]. PhC-based devices exhibit a smaller contrast ratio, which can arise when coupling strength is inadequate and loss is large [18]. Furthermore, PhC-based waveguides are more complex to fabricate in three dimensions, resulting in a much higher propagation loss than typical dielectric photonic waveguides [19]. Devices based on SOA have a restricted speed [20]. In the present manuscript, all-optical 1-bit FA has been designed employing two silicon MRRs only that has appealing aspects like large "quality factor", "ultrafast switching", "compact size", "improved bandwidth", "low power consumption", "ease in fabrication" etc. [21-22]. MRR-based devices work faster as the "carrier lifetime" is in picoseconds [23].

This is how the proposed manuscript is arranged. Section 1 describes the importance of AO technology and the previous work of AO 1-bit FA. The operation of the

MRR-based AO switch is demonstrated in section 2. One-bit FA based on MRR is elaborated in section 3. Section 4 covers MATLAB and FDTD simulation results of 1-bit FA. Section 5 assesses the important operational factors of the design and the conclusion is given in section 6.

## 2. Switching behaviour in MRR

An MRR includes 1 or 2 straight waveguides connected to a circle waveguide that is composed of 4 ports as depicted in Fig. 1 [22]. Optical input (I/P) is applied to “add port (AP)” and “input port (IP)”. Optical output (O/P) is received from “through port (TP)” and “drop port (DP)” of the MRR. A “continuous wave (CW) probe signal” (optical) is applied to IP of the MRR. “Probe signal” has no impact on the silicon as the strength is low. A strong optical signal is applied, either from upper side of

MRR or through the AP, to achieve the switching. The “ON resonance” of MRR takes place when the round-trip “optical path-length difference (OPD)” is equal to an integer multiple of resonant wavelength ( $\lambda_{res}$ ) of MRR. This moment, only DP gets the signal which was applied to IP. In the MRR, “two-photon absorption (TPA)” causes the generation of free carriers in response to a powerful pump signal. The “refractive index (RI)” of silicon MRR is changed by the “plasma-dispersion” effect [23]. The MRR will undergo a phase shift, causing the I/P signal to move from DP to TP. “Logic 0” (LOW) or “1” (HIGH) denote the absence or presence of a pump, respectively. Logically, DP and TP O/P are indicated by ‘ $\bar{Y}$ ’ and ‘ $Y$ ’, respectively, where pump is considered as variable ‘ $Y$ ’. TP and DP intensities are defined as below [22],

$$E_t = \frac{G\sqrt{1-k_1} - G\sqrt{1-k_2}x^2 \exp^2(j\phi)}{1 - \sqrt{1-k_1}\sqrt{1-k_2}x^2 \exp^2(j\phi)} E_{i1} + \frac{-G\sqrt{k_1}\sqrt{k_2}x \exp(j\phi)}{1 - \sqrt{1-k_1}\sqrt{1-k_2}x^2 \exp^2(j\phi)} E_{i2} \quad (1)$$

$$E_d = \frac{-G\sqrt{k_1}\sqrt{k_2}x \exp(j\phi)}{1 - \sqrt{1-k_1}\sqrt{1-k_2}x^2 \exp^2(j\phi)} E_{i1} + \frac{G\sqrt{1-k_2} - G\sqrt{1-k_1}x^2 \exp^2(j\phi)}{1 - \sqrt{1-k_1}\sqrt{1-k_2}x^2 \exp^2(j\phi)} E_{i2} \quad (2)$$

where,  $G = (1 - \gamma)^{1/2}$ ,  $x = G \exp(-\frac{\alpha L}{4})$ ,  $\phi = \frac{k_n L}{2}$ ,

$k_1$  is “coupling coefficient (CC)” between I/P waveguide and ring,  $k_2$  is CC between circular and O/P straight waveguide,  $k_n \left( \frac{2\pi}{\lambda_{res}} \cdot n_{eff} \right)$  is “wave propagation

constant”, “intensity attenuation factor” is  $\alpha$ , “intensity insertion loss coefficient” of coupler is  $\gamma$ , ring length is  $L$  ( $=29.845 \mu\text{m}$ ),  $E_{i1}$  is IP intensity and  $E_{i2}$  is AP intensity.

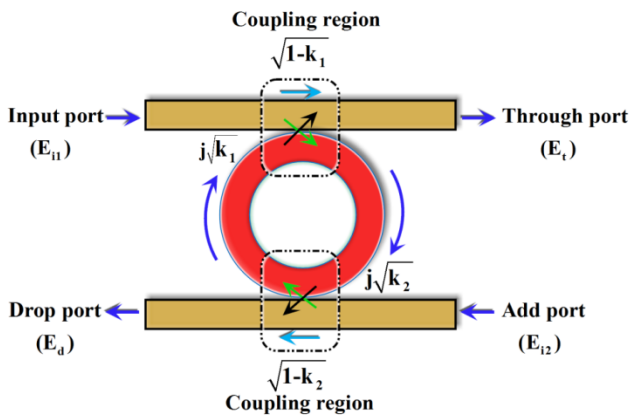


Fig. 1. Configuration of MRR (colour online)

The changing of RI of MRR upon powerful pump usage is shown by Eq. 3 and Eq. 4 [24],

$$\text{Phase shift, } \phi = \frac{2\pi}{\lambda} \cdot \Delta n L \quad (3)$$

where,

$$\Delta n = - \left[ 8.8 \times 10^{-22} \frac{\beta t_p^2}{2h\nu\sqrt{\pi\tau} S^2} P_{av}^2 + 8.5 \times 10^{-22} \left( \frac{\beta t_p^2}{2h\nu\sqrt{\pi\tau} S^2} P_{av}^2 \right)^{0.8} \right] \quad (4)$$

$P_{av}$  is “average pump power”,  $t_p$  ( $=3.75$  ps) is “pulse separation”,  $\tau$  ( $=200$  fs) is “pulse width”,  $h\nu$  is the “photon energy”, “TPA coefficient” is  $\beta$ . Change of phase vs “average power” of pump is shown in Fig. 2. Required average power is 0.97 mW for an MRR to cause  $\pi$ -phase shift. Alteration in DP and TP intensity w.r.t. wavelength are displayed in Fig. 3 in order to establish the connection between the output and Eqs.1-4.

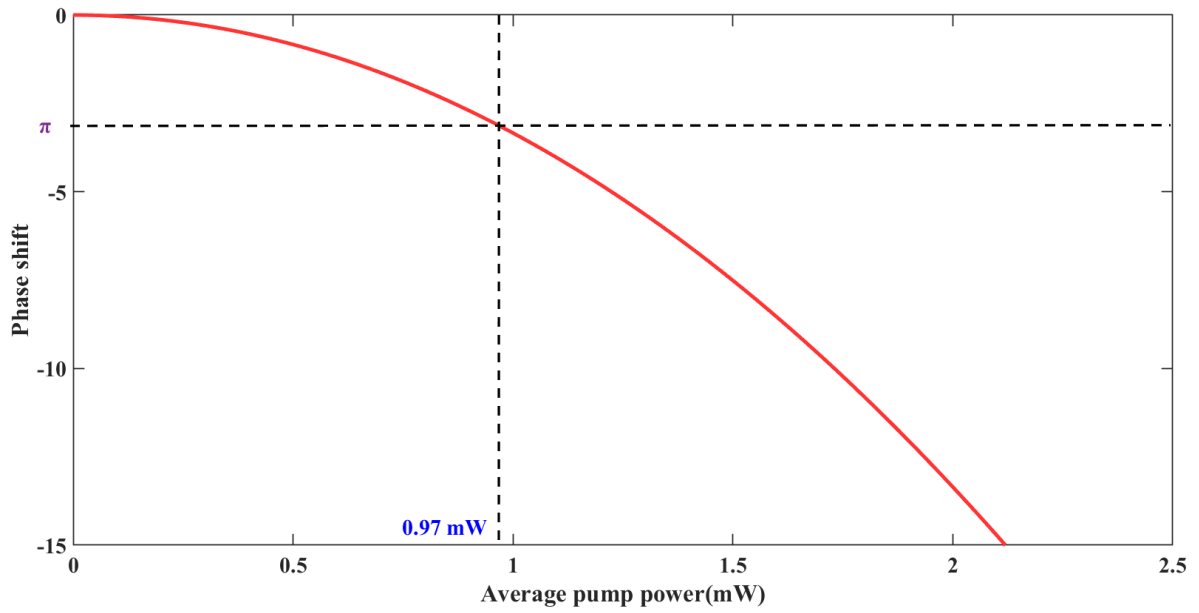
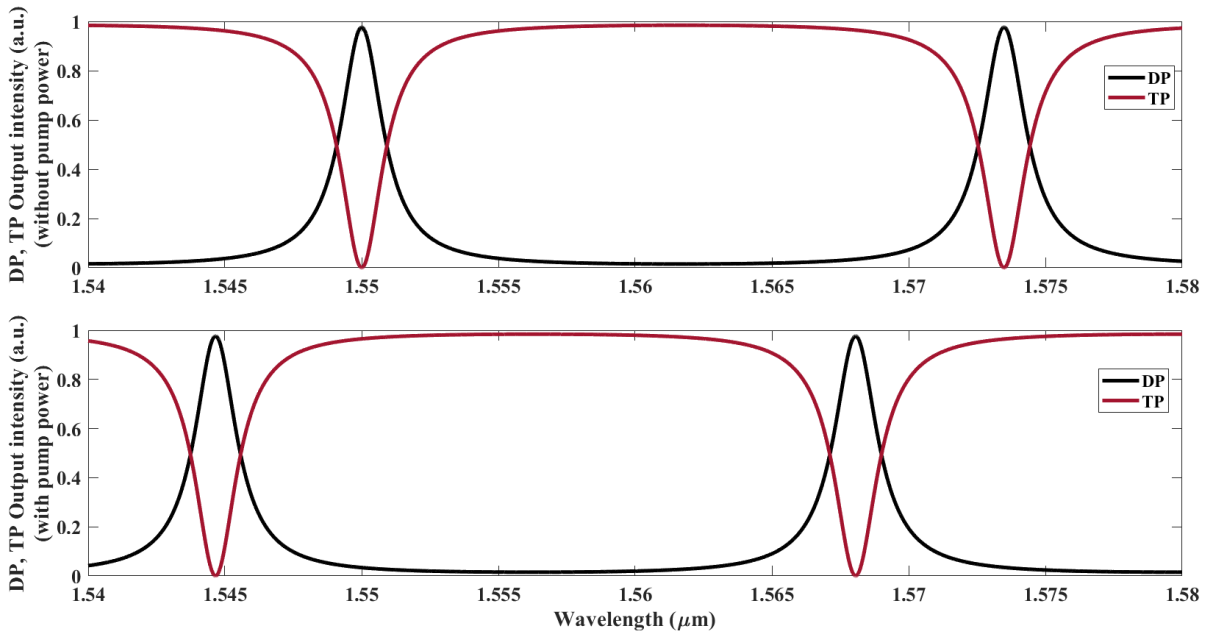

 Fig. 2. Phase change vs  $P_{av}$  (colour online)


Fig. 3. DP, TP intensity against wavelength (colour online)

### 3. MRR-based 1-bit full adder

An 1-bit FA has 3 I/Ps i.e. A, B and I/P carry ( $C_{in}$ ). Mathematically, the sum (SUM) and O/P carry ( $C_{out}$ ) can be expressed as [16],

$$SUM = A \oplus B \oplus C_{in} \quad (5)$$

$$C_{out} = AB + C_{in}(A \oplus B) \quad (6)$$

The related table for 1-bit FA is included in Table 1.

Table 1. Logic table of 1-bit FA

Inputs			Outputs	
A	B	Input carry, $C_{in}$	Sum (SUM)	Output carry, $C_{out}$
0	0	0	0	0
0	0	1	1	0
0	1	0	1	0
0	1	1	0	1
1	0	0	1	0
1	0	1	0	1
1	1	0	0	1
1	1	1	1	1

One-bit FA is designed using MRR-based 2-I/P XOR and AND gate that is covered in 3.1.

### 3.1. XOR and AND gate based on MRR

An essential part of implementing 1-bit FA is the XOR gate. O/P is “logic 0” when 2-I/Ps (A and B) are logically similar, else “logic 1”. Our previous work [22, 25] already demonstrated this, and it is depicted in Fig.4. Here, optical I/P works as “pseudo-pump”. The “resonance” of the MRR cannot be modified by a single I/P. Thus, “logic 0” is displayed by MRR’s TP, and “logic 1” by MRR’s DP. When, A and B are “logic 1”, MRR’s resonance shifts as the overall power of the I/Ps will be doubled. At this point, TP displays “logic 1” and DP displays “logic 0”. This operation satisfies the XOR and AND gate operation at DP and TP, respectively. Table 2 displays the associated truth table.

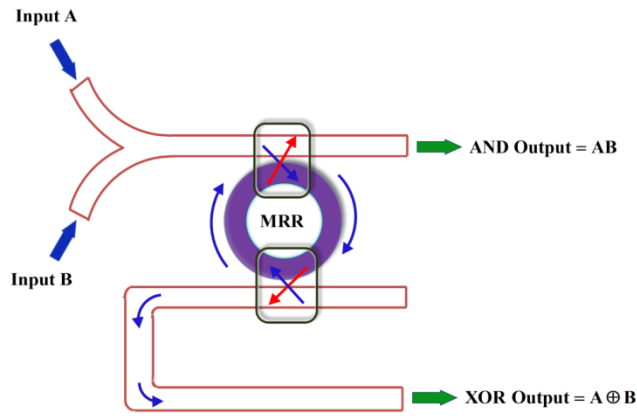


Fig. 4. XOR, AND gate based on MRR (colour online)

Table 2. Truth table of XOR and AND gate

Input A	Input B	Output at DP (XOR)	Output at TP (AND)
0	0	0	0
0	1	1	0
1	0	1	0
1	1	0	1

### 3.2. Implementation of 1-bit FA using MRR

MRR-based AO 1-bit FA has been depicted in Fig. 5. Here, we have employed two MRRs only, one beam combiner (BC) and one Erbium-doped waveguide amplifiers (EDWA).

#### 3.2.1. MRR1

The IP of MRR1 is optical data A and B. TP and DP outputs of MRR1 are  $AB$  and  $A \oplus B$ , respectively, in accordance with sub-section 3.1.

#### 3.2.2. MRR2

The XOR O/P of MRR1 acts as one of the I/P for MRR2. The other I/P for MRR2 is  $C_{in}$ . The DP of MRR1 is decreased due to some losses. In order to compensate for O/P of DP of MRR1, an EDWA, of the order of 3 dB, is employed in its path, and it makes use of silicon, the same WG material [26–27]. TP and DP of MRR2 are  $C_{in}(A \oplus B)$  and  $(A \oplus B \oplus C_{in})$ , respectively. BC is employed to combine optical TP output of MRR2 and MRR1, which is logically  $C_{out} = AB + C_{in}(A \oplus B)$ .

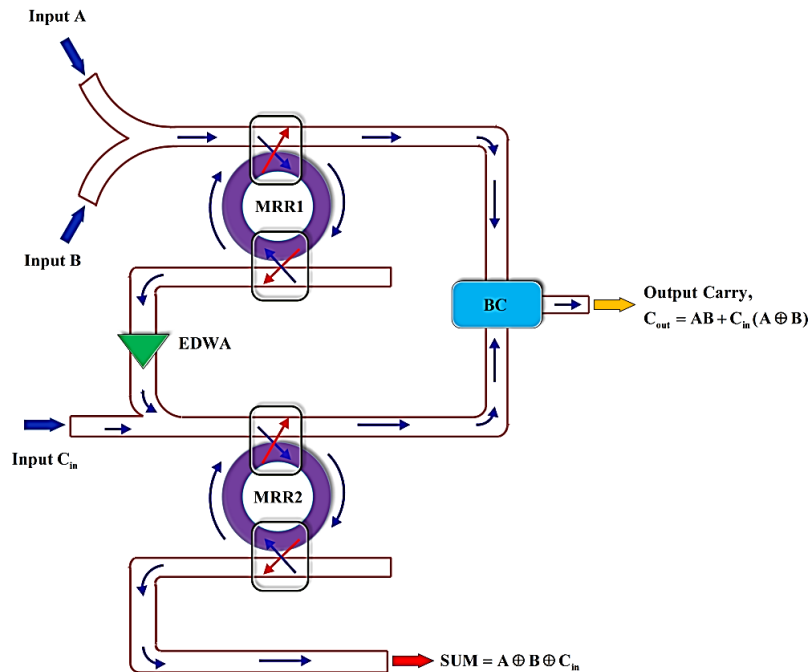


Fig. 5. MRR based 1-bit FA (colour online)

### 3.3. FDTD design of 1-bit FA using MRR

The MATLAB and FDTD simulation platforms have been used to implement 1-bit FA. Fig. 6 provides the equivalent FDTD simulation of the 1-bit FA. The footprint of the FDTD design is  $34.1 \mu\text{m} \times 32.2 \mu\text{m}$ . Below is a detailed discussion of how the MRR-based 1-bit FA operates.

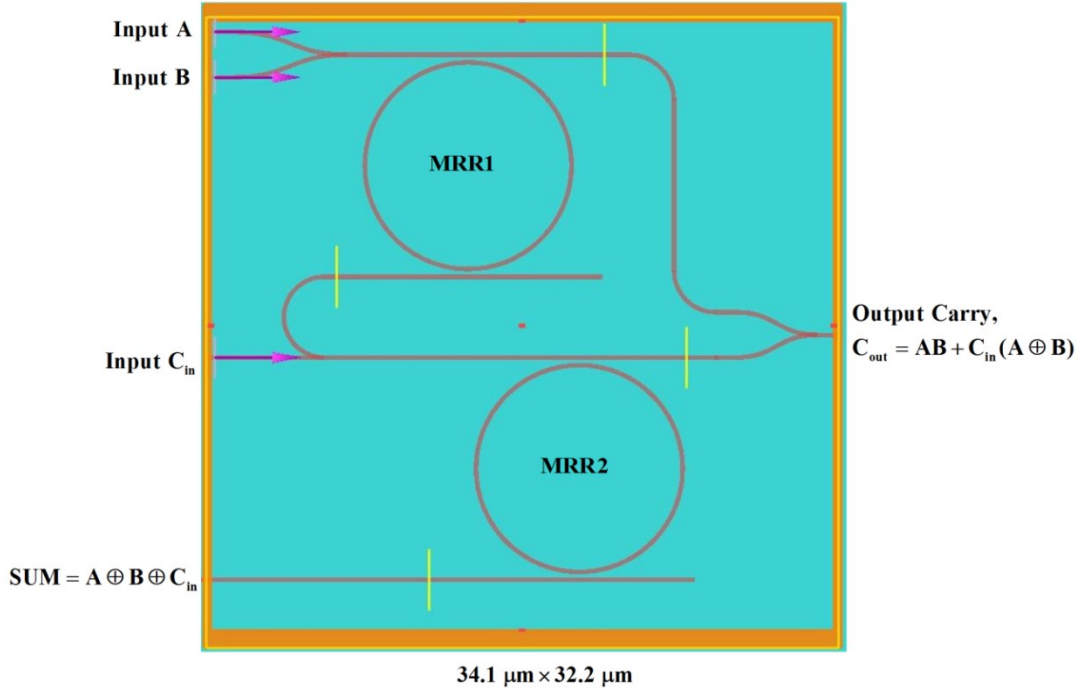


Fig. 6. FDTD schematics of 1-bit FA (colour online)

#### Case 2: (A, B, C<sub>in</sub> = 0, 0, 1)

Input A and B are “off” for MRR1. Input signal C<sub>in</sub> is “on” for MRR2. Both TP and DP of MRR1 are “logic 0” as I/P is absent to the MRR1. MRR2 has only one I/P. Respective TP and DP O/P of MRR2 are “logic 0” and “logic 1”. So, SUM = “logic 1” and C<sub>out</sub> = “logic 0”.

#### Case 3: (A, B, C<sub>in</sub> = 0, 1, 0)

Input A is “off” and B is “on” for MRR1. Input signal C<sub>in</sub> is “off” for MRR2. TP of MRR1 is “logic 0” and DP of MRR1 is “logic 1”. Only one input is there for MRR2. Respective TP and DP of MRR2 are “logic 0” and “logic 1”. So, SUM = “logic 1” and C<sub>out</sub> = “logic 0”.

#### Case 4: (A, B, C<sub>in</sub> = 0, 1, 1)

Input signal A is “off” and B is “on” for MRR1. Input signal C<sub>in</sub> is “on” for MRR2. TP of MRR1 is “logic 0”. DP of MRR1 is “logic 1”. Here, both I/Ps are present for MRR2, so TP is “logic 1”. DP of MRR2 is “logic 0”. BC O/P is “logic 1”. So, SUM = “logic 0” and C<sub>out</sub> = “logic 1”.

#### Case 1: (A, B, C<sub>in</sub> = 0, 0, 0)

Here, all I/Ps are “off”. So, there is no signal at the O/P of MRR2 and MRR1. As a result, SUM = “logic 0” and C<sub>out</sub> = “logic 0”.

#### Case 5: (A, B, C<sub>in</sub> = 1, 0, 0)

Input signal A is “on” and B is “off” for MRR1. Input signal C<sub>in</sub> is “off” for MRR2. Respective TP and DP of MRR1 are “logic 0” and “logic 1”. Only one input is there for MRR2. TP is “logic 0” and DP is “logic 1” for MRR2. So, SUM = “logic 1” and C<sub>out</sub> = “logic 0”.

#### Case 6: (A, B, C<sub>in</sub> = 1, 0, 1)

Input signal A is “on” and B is “off” for MRR1. Input signal C<sub>in</sub> is “on” for MRR2. Respective TP and DP are “logic 0” and “logic 1” for MRR1. As both I/Ps are present for MRR2, the respective TP and DP are “logic 1” and “logic 0” for MRR2. The BC O/P is “logic 1”. So, SUM = “logic 0” and C<sub>out</sub> = “logic 1”.

#### Case 7: (A, B, C<sub>in</sub> = 1, 1, 0)

Input signal A and B are “on” for MRR1. Input signal C<sub>in</sub> is “off” for MRR2. Here, both the I/Ps are present for MRR1. TP and DP of that ring are “logic 1” and “logic 0”, respectively. Both I/Ps are absent for MRR2, both TP and

DP are “logic 1” for MRR2. BC O/P is “logic 1”. So, SUM = “logic 0” and  $C_{out}$  = “logic 1”.

#### Case 8: (A, B, $C_{in}$ = 1, 1, 1)

Input signals A and B are “on” for MRR1. Input signal  $C_{in}$  is also “on” for MRR2. Here, both I/Ps are present for MRR1. Respective TP and DP are “logic 1” and “logic 0” for MRR1. In this case, only one input is present for MRR2. TP of MRR2 is “logic 0”. DP of MRR2 is “logic 1”. BC O/P is “logic 1”. So, SUM = “logic 1” and  $C_{out}$  = “logic 1”.

#### 4. Simulation

The MATLAB is utilized for simulation. Except for the MRR radius ( $4.75 \mu\text{m}$ ), the optimal settings are similar to those in [28]. Simulation of XOR, AND gate is represented in Fig. 7. One-bit FA simulation is depicted in Fig. 8. Ansys Lumerical FDTD is also used for the simulation of 1-bit FA. The intensity profile obtained in FDTD for different values of A, B and  $C_{in}$  is presented in Fig. 9.

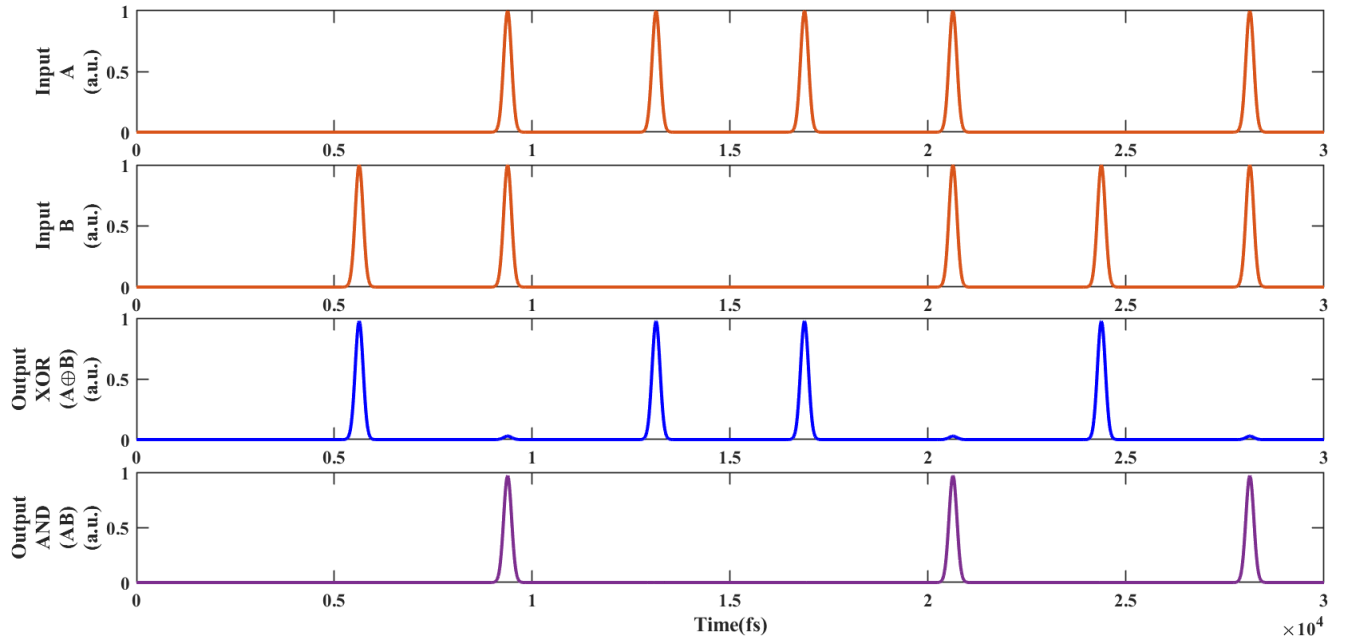


Fig. 7. XOR, AND gate simulation (colour online)

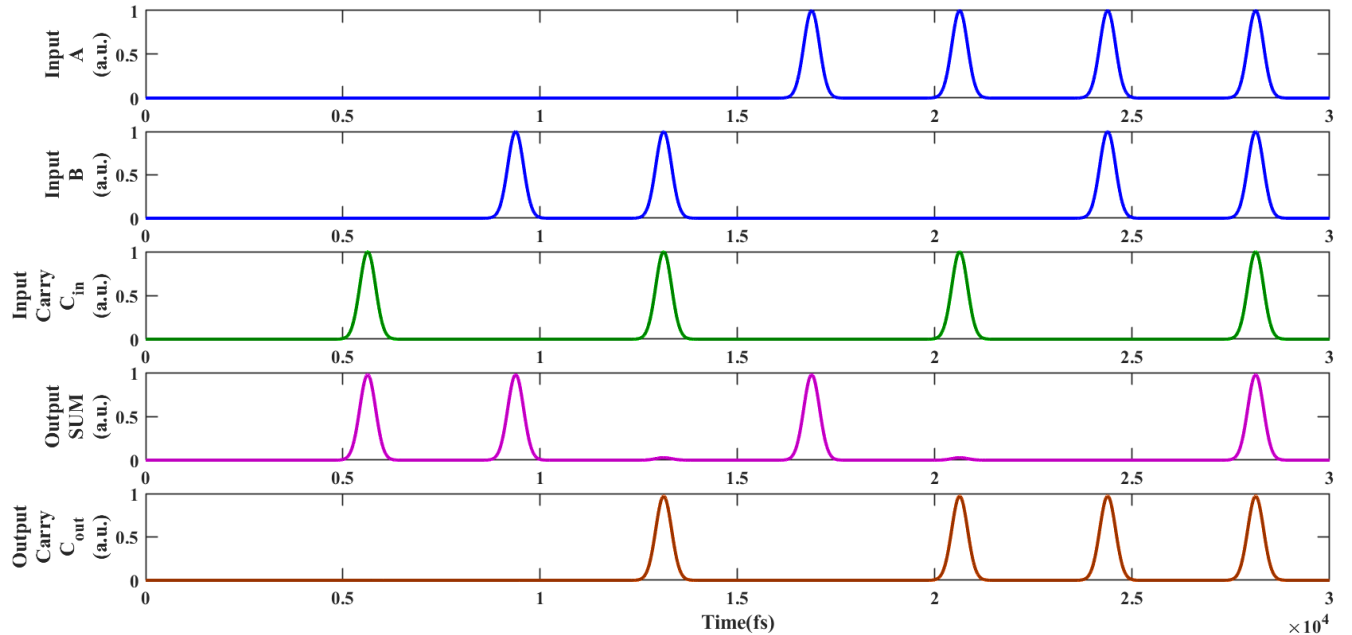


Fig. 8. Results of the simulation of 1-bit FA (colour online)

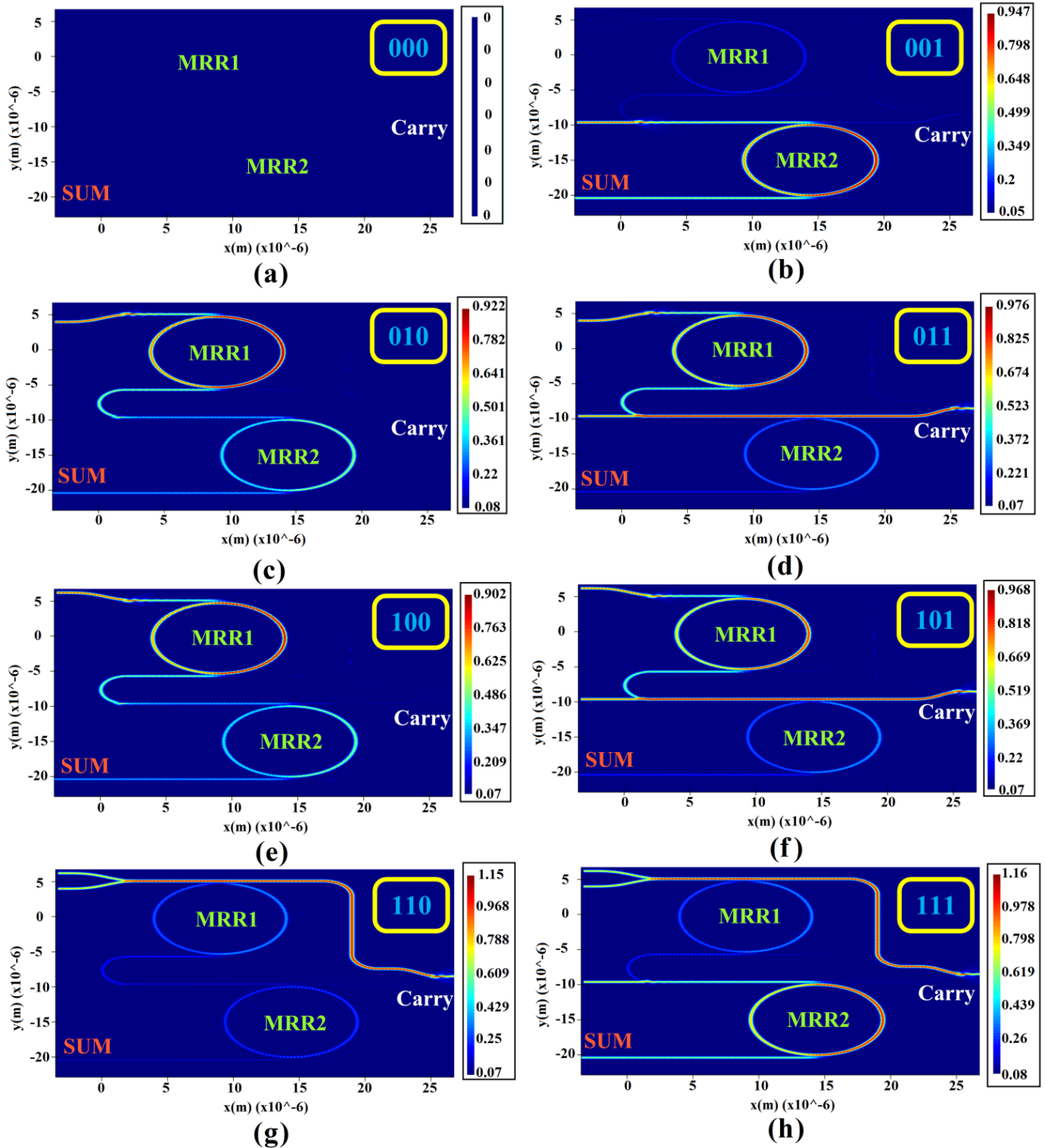


Fig. 9. Intensity profile of 1-bit FA (colour online)

## 5. Discussion

The CC and MRR radius should be suitably selected to operate an MRR as a switch. To select the value of CC, the value of the MRR radius and resonant wavelength ( $\lambda = 1.55 \mu\text{m}$ ) is kept at fixed values. Then, the CC is varied and check the difference between the maximum and minimum intensity for logic '1' and it has noticed that the smallest variation is obtained at the CC of 0.22 ( $k_1, k_2$ ). Also, the value of ER and CR is maximum at CC of 0.22

[29]. In the similar way, MRR radius ( $r = 4.75 \mu\text{m}$ ) is chosen where the CC is fixed at 0.22. So, the length of the MRR is  $L (2\pi r = 29.845 \mu\text{m})$ .

The "pulse width" and "pulse period" of the utilized signal decide how fast the proposed operates. This design uses "picosecond mode-locked fibre laser". Its "pulse duration" is 3.75 ps [30-31]. This is often referred to as the 3.75 ps MRR delay. The computed "switching speed" of the proposed design is  $(1/3.75) \text{ ps}$ , or around 260 Gbps. By

employing various “femtosecond lasers”, data speed can be improved [32-33].

Additionally, operational speed is influenced by “free carrier (photon) lifetime” in MRR. The “carrier lifetime ( $\tau_{cav}$ )” is expressed as [23],

$$\tau_{cav} = Q\lambda_{res}/(2\pi c) \quad (7)$$

where,  $c$  is “speed of light” (in vacuum),  $Q$  denotes “quality factor” of MRR, and  $\lambda_{res}$  denotes the “resonant wavelength”. The “full width at half maximum (FWHM)” and  $\lambda_{res}$  values are used to find  $Q$ . For the circuit we've described, the FWHM and  $\lambda_{res}$  values are 1.6 nm and 1550 nm, respectively. Attained value of  $Q$  is 968.  $\tau_{cav}$  is 0.8 ps, which is lesser than the “pulse duration” (3.75 ps). Quality factor,  $Q$  can be defined by,

$$Q = \lambda/\delta\lambda \quad (8)$$

where,  $\lambda$  is the resonant wavelength and  $\delta\lambda$  is the full width at half maximum (FWHM). If MRR length is increased, FWHM will be decreased and as a result,  $Q$  will be increased. But the optimized MRR length for the proposed design is of low value and that is why the quality factor is too low. However, we are not concerned about the  $Q$  for the proposed design.

Performance metrics must be measured for every design that is to be assessed for efficacy. “Extinction ratio (ER)”, “contrast ratio (CR)”, “amplitude modulation (AM)”, “on-off ratio (OOR)” and “pseudo eye diagram (PED)” are derived from the simulated results. To avoid interference, to improve “SNR”, and make it easier to identify resonance, AM must have lower value, while ER and CR must be of greater value. To guarantee that most of the I/P is transmitted toward the O/P, 10 dB CR and ER levels are adequate [34-35]. The AM, however, must be less than 1 dB [36].

The ER is expressed in dB as [28],

$$ER \text{ (dB)} = 10 \log\left(\frac{P_{min}^1}{P_{max}^0}\right) \quad (9)$$

where,  $P_{min}^1$  is “minimum” peak field for “logic 1” and  $P_{max}^0$  is “maximum” peak field for “logic 0”. ER vs. CCs is plotted at the same radius (4.75  $\mu\text{m}$ ) which is demonstrated in Fig. 10 (a). Likewise, ER vs. MRR radiuses is plotted at the same CC and depicted in Fig. 10 (b). ER of the design being proposed is 15.26 dB.

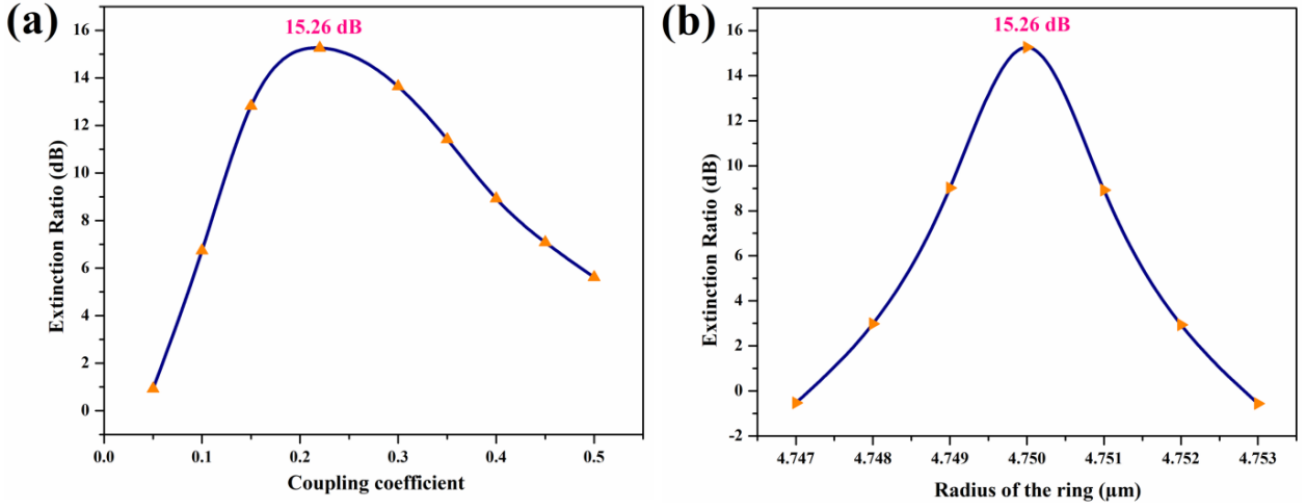


Fig. 10. ER against (a) CCs (b) MRR radiuses (colour online)

Proportion of mean O/P field for “logic 1” ( $P_{mean}^1$ ) and mean O/P field for “logic 0” ( $P_{mean}^0$ ) is CR [28],

$$CR \text{ (dB)} = 10 \log\left(\frac{P_{mean}^1}{P_{mean}^0}\right) \quad (10)$$

Fig. 11 (a) shows the plot CR vs. CCs where radius (4.75  $\mu\text{m}$ ) is unchanged and Fig. 11 (b) shows the plot CR vs. MRR radiuses with unchanged CC (0.22). At optimum values, CR is 21.24 dB.

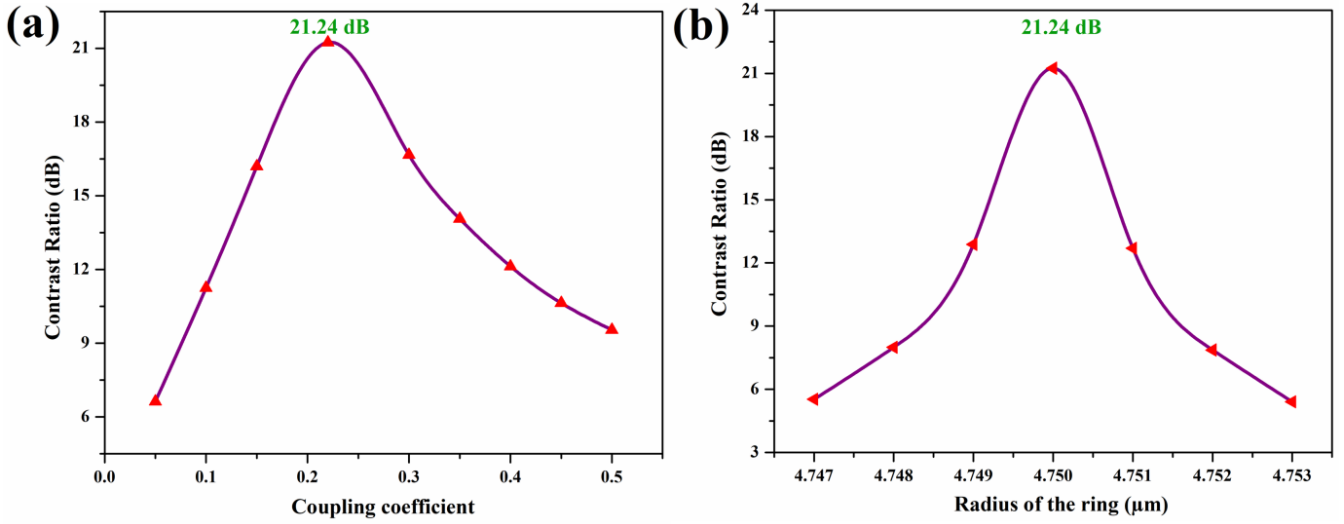


Fig. 11. CR against (a) CC (b) MRR radiuses (colour online)

The AM is computed as [28] in decibels,

$$AM \text{ (dB)} = 10 \log\left(\frac{P_{\max}^1}{P_{\min}^1}\right) \quad (11)$$

where,  $P_{\max}^1$  is “maximum” O/P for “logic 1”. Fig. 12 (a) exhibits AM vs. CCs at the same radius (4.75 μm). AM vs. MRR radiuses where CC is fixed and it is plotted in Fig. 12 (b). AM is 0.026 dB.

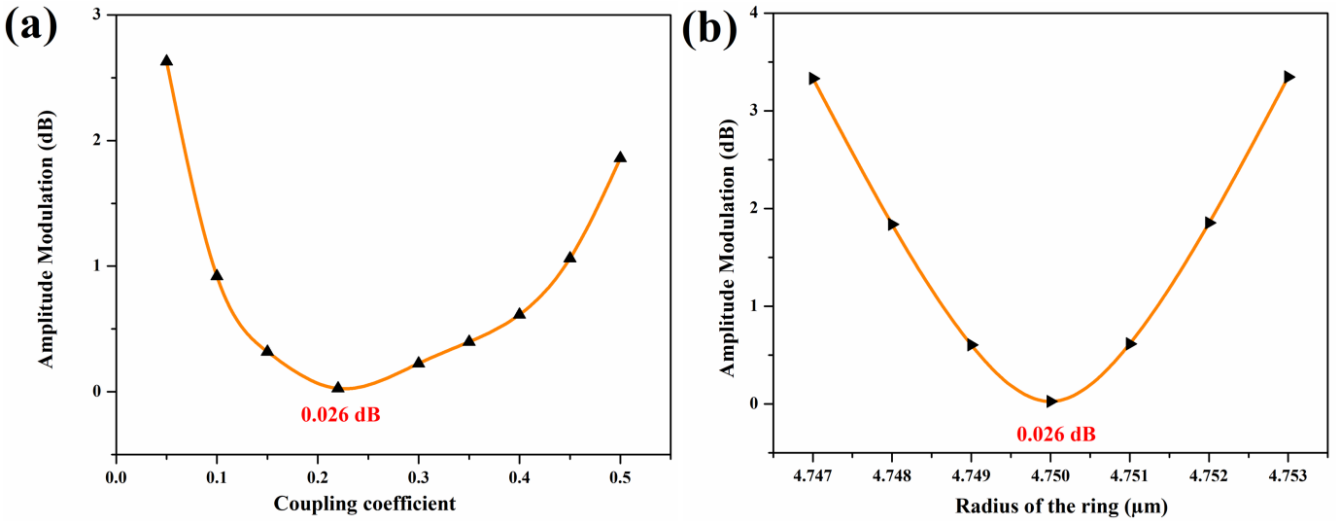


Fig. 12. AM vs. (a) CC (b) ring radii (colour online)

OOR is assessed by the proportion of “drop port” ( $T_{\max}$ ) and “through port” ( $T_{\min}$ ) value at resonance [28],

$$OOR = \frac{T_{\max}(DP)}{T_{\min}(TP)} \quad (12)$$

Having an OOR higher than 20 dB is necessary to operate with effectiveness for the design [37]. Fig. 13 shows the OOR, which is 38.43 dB.

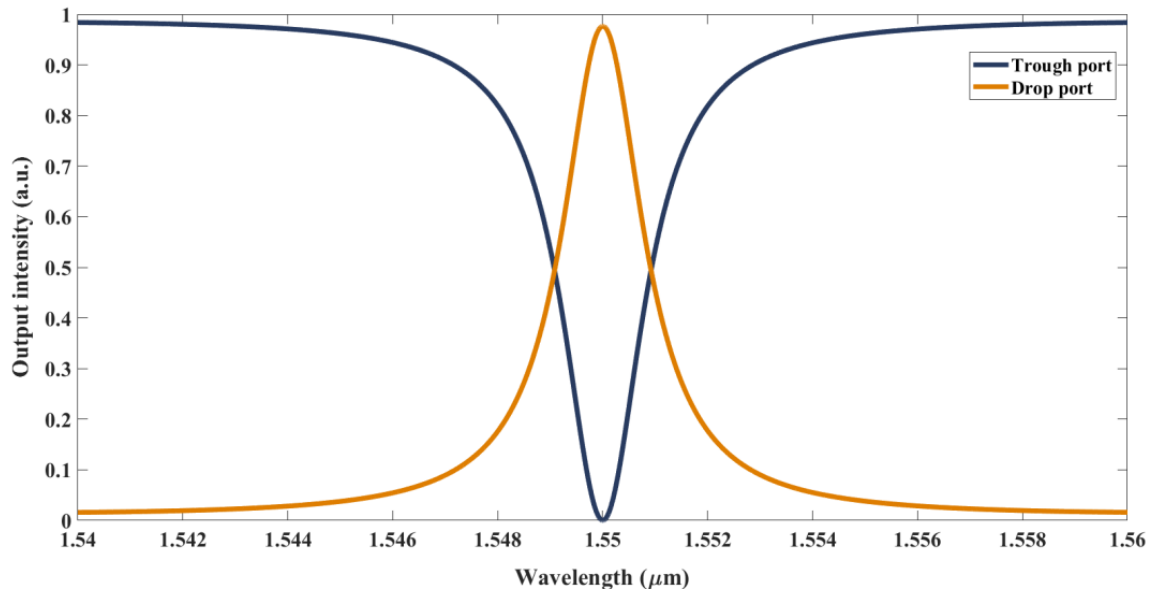


Fig. 13. On-off ratio (colour online)

Another significant parameter is the “pseudo eye diagram (PED)” [28]. The PED for 1-bit FA is shown in Fig. 14. Every possible O/P for “logic 0” and “logic 1” is superimposed to represent PED. The envelopes of “logic 0” and “logic 1” may clearly be differentiated. “Relative eye opening ( $O$ )” is an additional component of PED quality [28],

$$O = \frac{(P_{\min}^1 - P_{\max}^0)}{P_{\min}^1} \quad (13)$$

$O = 97.02\%$  for 1-bit FA.

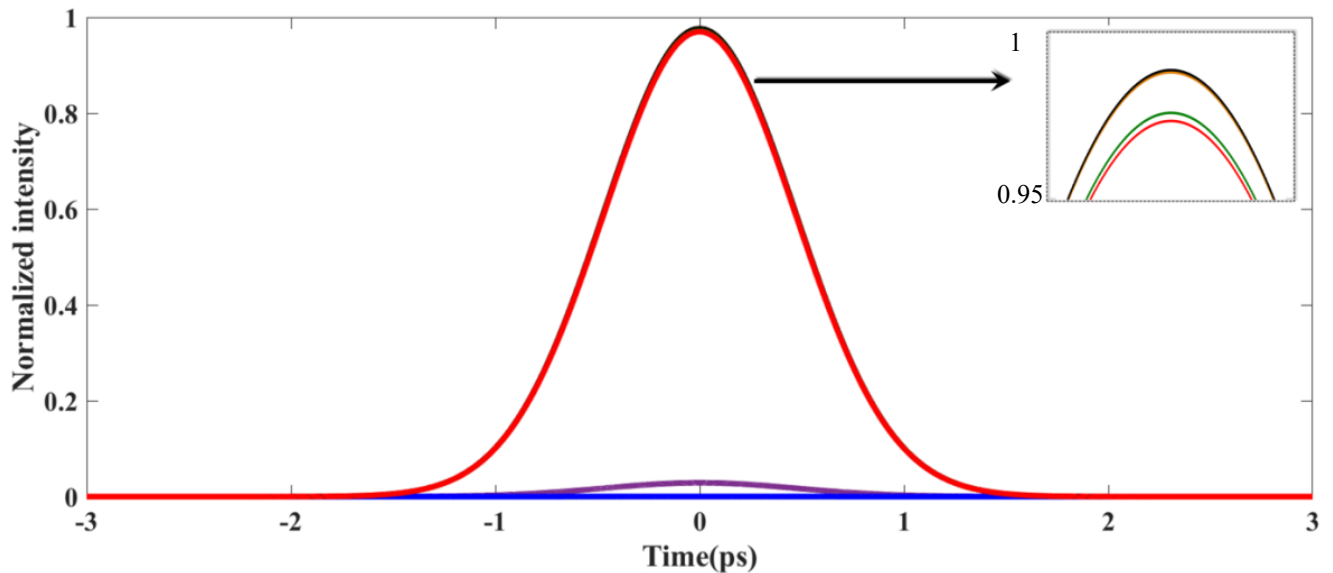


Fig. 14. PED for 1-bit FA (colour online)

## 6. Conclusion

In conclusion, one-bit FA has been deployed using two MRRs only. All-optical 1-bit FA is theoretically implemented and analyzed. MATLAB and FDTD software obey the related table of 1-bit FA. To induce the

switching phenomena, an MRR needs just 0.97 mW of pump power. Moreover, the suggested design might operate at around 260 Gbps. CR and ER are 21.24 dB and 15.26 dB, respectively. AM is 0.026 dB, which is less than 1 dB. The OOR is 38.43dB. Obtained Q factor is 968. For 1-bit FA, the “relative eye opening” is 97.02%.

**Declaration:**

**Funding:** There was no funding for this research project

**Conflict of Interest:** The authors have declared no conflict of interest.

**Code and Data Availability Statement:** Data sharing is not applicable to this article, as no new data were created or analyzed.

**Authors' Contributions:**

**Bhuvaneswari Viswanathan-** Methodology, implementation, simulation and writing original draft preparation.

**Yuvaraj Sivagnanam-** Supervision, reviewing and editing the draft manuscript.

**Jayanta Kumar Rakshit -** Simulation, reviewing and editing the draft manuscript.

**Manjur Hossain -** Conceptualization, supervision, reviewing and editing the draft manuscript.

**References**

- [1] C. Qiu, C. Zhang, H. Zeng, T. Guo, *Journal of Lightwave Technology* **39**(7), 2099 (2020).
- [2] A. Raja, K. Mukherjee, J. N. Roy, *Journal of Computational Electronics* **20**, 387 (2021).
- [3] K. Mukherjee, *Optics & Laser Technology* **140**, 107043 (2021).
- [4] K. Maji, K. Mukherjee, M. K. Mandal, *Journal of Nonlinear Optical Physics & Materials* **32**(04), 2350034 (2023).
- [5] J. Gosciniak, Z. Hu, M. Thomaschewski, V. J. Sorger, J. B. Khurgin, *Laser & Photonics Reviews* **17**(4), 2200723 (2023).
- [6] M. P. Singh, J. K. Rakshit, M. Hossain, *Optical and Quantum Electronics* **53**(12), 703 (2021).
- [7] M. Hossain, J. K. Rakshit, A. Bhatnagar, T. Chattopadhyay, *Optik* **282**, 170891 (2023).
- [8] M. P. Singh, M. Hossain, J. K. Rakshit, G. K. Bharti, J. N. Roy, *Brazilian Journal of Physics* **51**(6), 1763 (2021).
- [9] A. Kumar, M. Kumar, S. K. Jindal, S. K. Raghuvanshi, R. Choudhary, *Optical and Quantum Electronics* **53**, 1 (2021).
- [10] K. K. Choure, A. Saharia, N. Mudgal, R. Pandey, A. Agarwal, M. Prajapat, R. Maddila, M. Tiwari, G. Singh, *Optics Communications* **530**, 129126 (2023).
- [11] A. Saharia, N. Mudgal, K. K. Choure, R. Maddila, M. Tiwari, G. Singh, *Optik* **251**, 168493 (2022).
- [12] A. M. Vali-Nasab, A. Mir, R. Talebzadeh, *Optical and Quantum Electronics* **51**, 1 (2019).
- [13] M. J. Maleki, A. Mir, M. Soroosh, *Optical and Quantum Electronics* **52**, 1 (2020).
- [14] M. J. Maleki, A. Mir, M. Soroosh, *Optik* **227**, 166107 (2021).
- [15] S. Kaur, R. S. Kaler, T. S. Kamal, *Journal of the Optical Society of Korea* **19**(3), 222 (2015).
- [16] P. K. Nahata, A. Ahmed, S. Yadav, N. Nair, S. Kaur, **2020** 7th International Conference on Signal Processing and Integrated Networks (SPIN), IEEE, 1044 (2020).
- [17] F. Chen, S. Zhou, Y. Xia, X. Yu, J. Liu, F. Li X. Sui, *Applied Optics* **63**(1), 147 (2024).
- [18] B. E. Little, S. T. Chu, W. Pan, D. Ripin, T. Kaneko, Y. Kokubun, E. Ippen, *IEEE Photonics Technology Letters*, **11**(2), 215 (1999).
- [19] L. Gan, Z. Li, *Science China Physics, Mechanics & Astronomy* **58**, 1 (2015).
- [20] C. Qin, X. Huang, X. Zhang, *IEEE Journal of Quantum Electronics* **47**(11), 1443 (2011).
- [21] R. Soref, *IEEE Journal of Selected Topics in Quantum Electronics* **12**(6), 1678 (2006).
- [22] J. K. Rakshit, M. Hossain, *Photonic Network Communications* **44**(2-3), 116 (2022).
- [23] Q. Xu, M. Lipson, *Optics Express* **15**(3), 924 (2007).
- [24] L. Chun-Fei, D. Na, *Chinese Physics Letters* **26**(5), 054203 (2009).
- [25] V. Magesh, J. Shirisha, K. Lavanya, M. Hossain, *Optical and Quantum Electronics* **56**(7), 1200 (2024).
- [26] G. K. Bharti, R. K. Sonkar, *Optical and Quantum Electronics* **54**(3), 176 (2022).
- [27] L. Agazzi, J. D. Bradley, M. Dijkstra, F. Ay, G. Roelkens, R. Baets, K. Wörhoff, M. Pollnau, *Optics Express* **18**(26), 27703 (2010).
- [28] M. Hossain, K. Mondal, D. Kumar, J. K. Rakshit, S. Mandal, *Optical and Quantum Electronics* **55**(12), 1100 (2023).
- [29] J. K. Rakshit, T. Chattopadhyay, J. N. Roy, *Optik* **124**(23), 6048 (2013).
- [30] P. Deslandes, M. Perrin, J. Saby, D. Sangla, F. Salin, E. Freysz, *Optics Express* **21**(9), 10731 (2013).
- [31] L. Duan, M. Dagenais, J. Goldhar, *Journal of Lightwave Technology* **21**(4), 930 (2003).
- [32] F. Krausz, M. E. Fermann, T. Brabec, P. F. Curley, M. Hofer, M. H. Ober, C. Spielmann, E. Wintner, A. J. Schmidt, *IEEE Journal of Quantum Electronics* **28**(10), 2097 (1992).
- [33] W. Sibbett, A. A. Lagatsky, C. T. A. Brown, *Optics Express* **20**(7), 6989 (2012).
- [34] C. Y. Chao, L. J. Guo, *Journal of Lightwave Technology* **24**(3), 1395 (2006).
- [35] A. K. Dutta, N. K. Dutta, M. Fujiwara, *WDM Technologies: Passive Optical Components*, Academic Press, 379 (2003).
- [36] J. S. Vardakas, K. E. Zoiros, *Opt. Eng.* **46**(8), 085005 (2007).
- [37] D. G. Rabus, M. Hamacher, U. Troppenz, H. Heidrich, *IEEE Photonics Technology Letters* **14**(10), 1442 (2002).

\*Corresponding author: manjurhossain2003@gmail.com